International Journal of Power Electronics and Drive System (IJPEDS)
Vol. 17, No. 2, June 2026, pp. 1475~1485
ISSN: 2088-8694, DOI: 10.11591/ijpeds.v17.i2.pp1475-1485

Super-twisting MPPT enhanced via grey wolf optimization for dynamic PV operation

Slimane Hadji[1], Said Aissou[2], Abdelhakim Belkaid[1]
[1]Laboratoire de Technologie Industrielle et de l'Information (LTII), Faculté de Technologie, Université de Bejaia, Bejaia, Algérie
[2]Laboratoire de Maitrise des Energies Renouvelables (LMER), Faculté de Technologie, Université de Bejaia, Bejaia, Algérie

Article Info

Article history:

Received Dec 7, 2025
Revised Apr 19, 2026
Accepted May 5, 2026

Keywords:

Energy efficiency
Grey wolf optimizer
Maximum power point
Photovoltaic systems
Super twisting algorithm
Tracking

ABSTRACT

This paper introduces a hybrid maximum power point tracking (MPPT) strategy for photovoltaic (PV) systems under rapidly varying irradiance conditions. The approach combines the super-twisting algorithm (STA), a second-order sliding mode control technique, with the grey wolf optimizer (GWO) in a coordinated framework where control action and parameter adaptation are jointly addressed. Unlike conventional MPPT methods that treat control and optimization separately, the proposed scheme improves transient response while limiting steady-state oscillations. The method is evaluated through MATLAB/Simulink simulations under multiple dynamic irradiance profiles, including fast-changing environmental conditions. Performance is assessed using complementary metrics, namely tracking efficiency, convergence dynamics, and root mean square error (RMSE), to provide an objective analysis. Results show that the STA-GWO strategy achieves faster convergence and improved stability compared to conventional SMC-GWO. It reaches an average tracking efficiency of 99.34%, compared to 99.19% for SMC-GWO, with reduced power fluctuations reflected by a lower RMSE. These improvements indicate a better trade-off between dynamic performance and steady-state accuracy. While this study is based on simulations, its findings require experimental validation. Future work will therefore include real-time implementation to confirm the practical applicability of the proposed approach.

Corresponding Author:

Said Aissou
Laboratoire de Maitrise des Energies Renouvelables (LMER), Faculté de Technologie, Université de Bejaia Bejaia, Algérie
Email: said.aissou@univ-bejaia.dz

1. INTRODUCTION

Solar energy, with its abundance and low carbon footprint, is central to the global energy transition [1]-[3]. Photovoltaic (PV) systems are strongly influenced by irradiance and temperature variations, which cause fluctuations in power output. To address this, maximum power point tracking (MPPT) algorithms are employed to continuously optimize operating conditions and maximize energy extraction [4], [5]. Conventional methods such as perturb and observe (P&O) and incremental conductance (INC) have been widely used due to their simplicity and low cost, though they face limitations under rapidly changing weather conditions.

The P&O algorithm perturbs the operating point to detect power variations and adjust voltage, but it suffers from oscillations around the maximum power point (MPP) and slow convergence under rapid irradiance changes [6], [7]. The incremental conductance (INC) method improves accuracy by exploiting the power–voltage derivative, yet remains sensitive to noise.

These limitations have driven the development of advanced MPPT strategies based on artificial intelligence and metaheuristic optimization, offering enhanced tracking speed, stability, and robustness. Fuzzy logic has been widely applied in MPPT due to its ability to manage uncertainty and adapt to environmental changes. However, despite this performance, it requires optimization to improve robustness [5]. Artificial neural networks (ANNs) offer another promising solution by leveraging learning capabilities to predict the MPP [1]. However, ANN deployment demands high computational resources, which limits their use in low-power embedded systems. Meanwhile, metaheuristic algorithms have gained popularity due to their efficiency. Among these techniques, particle swarm optimization (PSO) has been widely applied to MPPT because of its fast convergence and robustness against environmental disturbances [8], [9]. Hybrid approaches, such as PSO-P&O, improve both stability and tracking accuracy. Other metaheuristic algorithms, including ant colony optimization (ACO) [10], [11], grey wolf optimization (GWO) [12], [13], and differential evolution (DE), have also been investigated, each offering distinct advantages in terms of robustness, convergence speed, and computational efficiency.

Recent studies propose hybrid methods to further enhance MPPT performance, such as ANFIS–PSO and fuzzy logic–GWO [14], which improve adaptability and power extraction under variable conditions. Sliding mode control (SMC) has also been explored for its disturbance rejection, though its chattering effect induces oscillations and energy losses. The super-twisting algorithm (STA) mitigates this drawback, improving stability and efficiency in SMC-based MPPT [15], [16]. Despite these advances, extensive validation under real-world conditions remains necessary.

This study presents a comprehensive assessment of two MPPT techniques, SMC-GWO and STA-GWO, with a particular emphasis on their performance under dynamically varying irradiance and temperature conditions. Using MATLAB/Simulink simulations, using MATLAB/Simulink simulations, this study provides valuable insights into the efficiency of the proposed MPPT algorithms, highlighting the strengths of the combined approach under various operating conditions. However, a key limitation of this work lies in the absence of a hardware-in-the-loop (HIL) implementation, which remains a direction for future work.

2. SYSTEM DESCRIPTION AND MODELLING

Photovoltaic power generation is strongly affected by meteorological conditions, with solar irradiance being the dominant factor. While manufacturers specify module parameters under standard test conditions (STC), real-world operation rarely matches these ideal values. Low irradiance can force the system to it short-circuit current when load demand exceeds module capacity, causing failure. To ensure stable operation, load–generator decoupling is required, achieved through power electronics. DC/DC converters with MPPT enable efficient adaptation, with Boost-type converters (non-isolated step-up) widely used in research for raising the low voltage of PV panels. Figure 1 shows a PV system architecture employing a boost converter for decoupling.

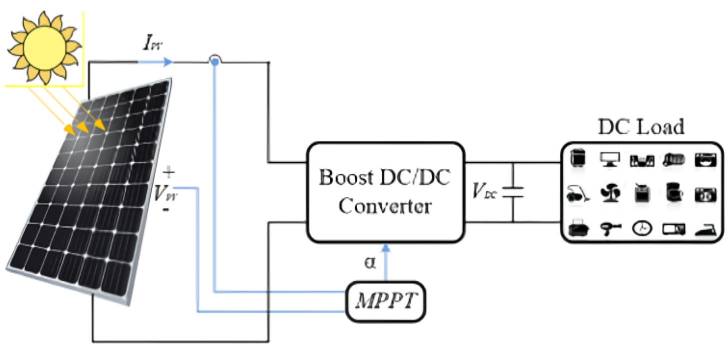

Figure 1. Illustration of the PV system under study

2.1. PV model modeling

The photovoltaic single-diode equivalent circuit model, as shown in Figure 2, is widely adopted for PV cell modelling because of its simplicity and satisfactory accuracy. The model utilized in this study is the same as the one used in previous research [9], [10], [17].

In accordance with Kirchhoff's theorem applied to the presented model, the currents within the photovoltaic cell can be expressed as (1) [5], [11].

$$I_{PV} = I_{ph} - I_d - I_{Rsh} \tag{1}$$

Where: I_{ph}, the photo-current, I_d the diode-current and I_{Rsh} the shunt current [18]-[21]. After substituting the currents I_d and I_{Rsh} with their expressions in (1), photovoltaic current is obtained as expressed in (2) [11], [13].

$$I_{PV} = I_{ph} - I_0 \cdot \left[exp\left(\frac{q\cdot(V_{PV}+R_S\cdot I_{PV})}{A\cdot N_S\cdot K\cdot T_j}\right) - 1\right] - \frac{V_{PV}+R_S\cdot I_{PV}}{R_{sh}} \tag{2}$$

Table 1 presents the photovoltaic panel parameters.

The (1) and (2) represent a mathematical model of a PV panel, able to describe the behavior of the module in Simulink. Several simulations were carried out. Figure 3 illustrates the characteristics obtained under varying levels of solar irradiance, ranging from 1000 W/m² with an increment of 200 W/m². The maximum power points are indicated by red asterisks (*).

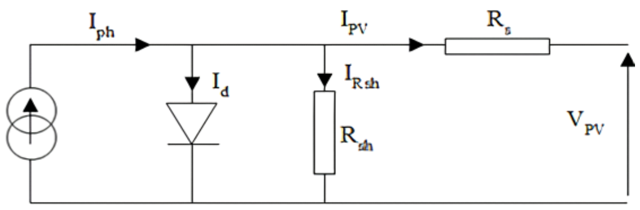

Figure 2. Equivalent circuit of solar cell

Table 1. Photovoltaic panel parameters

Symbol	Parameters	Values
P_{pv}	Photovoltaic power	80 Wp
I_{mppt}	Maximum current at MPP	4.65 A
V_{mppt}	Maximum voltage at MPP	17.5 V
I_{sc}	Short circuit current	4.95 A
V_{oc}	Open circuit voltage	21.9 V
α_{sc}	Temperature coefficient at short-current	3 mA/°C
β_{oc}	Voltage temperature coefficient of short-current	150 mV/°C

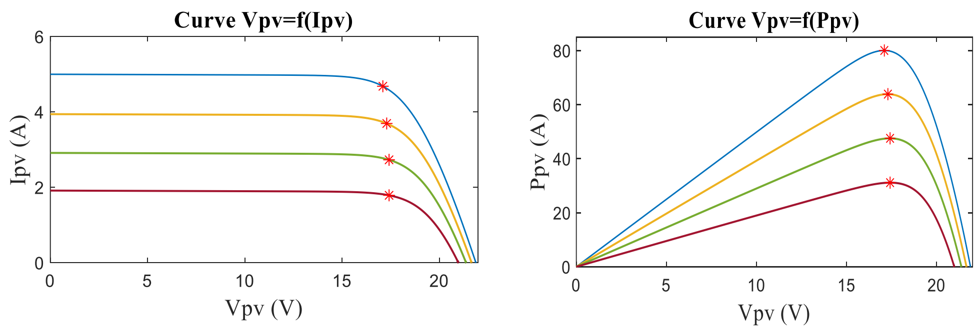

Figure 3. Electrical IV and PV curves for photovoltaic panel STP80

2.2. DC-DC converter

In power electronics, DC–DC converters regulate average DC signals via duty cycle of the switching device. Within PV systems, they act as adaptation interfaces, adjusting voltage and current to track the MPP and avoid short-circuit operation. Figure 4 shows the boost converter topology commonly used for PV panels. When the IGBT/MOSFET is ON, the source charges the inductor while the diode is reverse-biased. When the switch is OFF, both the inductor and source deliver energy to the load. The input–output voltage and current relationships are defined by (3) [2], [5].

$$V_{out} = \frac{V_{in}}{(1-\mathrm{D})}$$
$$I_{in} = \frac{I_{out}}{(1-D)} \quad (3)$$

The dynamic equations of this converter as (4) to (6) [22], [23].

$$\begin{pmatrix} \frac{dI_L}{dt} = \frac{V_{pv}-V_0}{L} + \frac{V_0}{L}u \\ \frac{dV_0}{dt} = \left(-\frac{V_0}{RC} + \frac{I_L}{C}\right)\frac{V_0}{L}u \end{pmatrix} \quad (4)$$

$$\dot{X} = f(X) + b(X)u \quad (5)$$

$$f(X) = \begin{bmatrix} \frac{V_{pv}-V_0}{L} \\ \frac{-V_0}{RC} + \frac{I_L}{C} \end{bmatrix} \; and \;\; b(X) = \begin{bmatrix} \frac{V_0}{L} \\ \frac{-V_0}{C} \end{bmatrix} \quad (6)$$

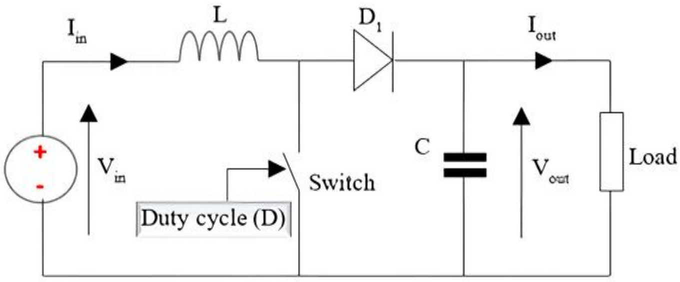

Figure 4. The power circuit of a DC-DC boost converter

2.3. MPPT controller
2.3.1. Super-twisting sliding mode control for MPPT

The super-twisting algorithm is an advanced form of SMC designed to suppress chattering, thereby improving the durability and efficiency of PV systems. Using a nonlinear control law, it reduces switching effort and enhances dynamic response. In environments with variable irradiance and temperature, the controller ensures robust MPPT. Its implementation involves two stages: i) defining a sliding surface based on system dynamics to guarantee fast and stable convergence, and ii) designing a control law comprising equivalent and switching actions that constrains system states to the surface. Embedded in an adaptive feedback loop, the method minimizes disturbances, reduces oscillations, and improves both efficiency and reliability of PV systems [2].

– Sliding surface

According to the literature, a selection of sliding surfaces has been employed by researchers [1]. The sliding surface S(x,t) is chosen according to (7). Both it and the first derivative should be zero. The sliding surface proposed in [7] is chosen to validate that the system attains the MPP.

$$s^{\cdot}(x,t) = 0 \; s(x,t) = \frac{\partial P_{pv}}{\partial V_{pv}} = V_{pv}\left(\frac{\partial I_{pv}}{\partial V_{pv}} + \frac{I_{pv}}{V_{pv}}\right) = 0 \quad (7)$$

– Control law design

The SMC signal is composed of two distinct components, each fulfilling a critical role in ensuring robust and precise MPPT operation. The first component, the equivalent control, continuously adjusts system dynamics to maintain adherence to the sliding surface. By ensuring a smooth and stable response, it stabilizes the system under normal conditions and optimizes PV performance by accurately tracking the MPP despite variations in irradiance and temperature. The second component, the switching control, counteracts disturbances and model uncertainties by applying a discontinuous control action that redirects the system state toward the sliding surface whenever deviations occur. This mechanism enhances system resilience by swiftly correcting off-surface excursions, ensuring robustness against external perturbations.

The synergy between equivalent and switching controls makes SMC highly effective in dynamic and uncertain environments. While the equivalent control maintains operational stability and efficiency, the switching control guarantees rapid disturbance rejection. This dual-component design is integral to advanced MPPT strategies, enabling consistent MPP tracking and maximizing energy harvesting in PV systems. Figure 5 provides the structure of the ST-SMC method [3]. The global system equation control is given in (8).

$$U = U_{sc} + U_{ec} \tag{8}$$

Where, U_{ec} equivalent control and U_{sc} *is* switching control, the equation of switching control is given in (9).

$$U_{sc} = U_1 + U_2 \tag{9}$$

The equations of U_1 and U_2 is given in (10).

$$\dot{U}_1 = -\gamma . sign\ (S)\ and\ U_2 = -\lambda . |S|^{\frac{1}{2}}\ sign\ (S) \tag{10}$$

Where γ and λ are design parameters, their respective equations are given by (11).

$$\gamma > \frac{\Phi}{\Gamma_m}\ and\ \lambda > \sqrt{\frac{2}{\Gamma_m^2} . \frac{(\Gamma_m \gamma + \Phi)^2}{\Gamma_m \gamma - \Phi}} \tag{11}$$

The (12) provides the equivalent control U_{ec}.

$$U_{ec} = -\frac{\left[\frac{dS}{dX}\right]^T f(X)}{\left[\frac{dS}{dX}\right]^T b(X)} = 1 - \frac{V_{pv}}{V_0} \tag{12}$$

The next step involves deriving and demonstrating the stability conditions to ensure the system operates within desired parameters.

– Stability analysis

The Lyapunov function is defined to ensure the stability of the suggested controller, as detailed in (13) and (14).

$$\mathrm{V(t)} = \frac{1}{2}\ \mathrm{S}^2\mathrm{(t)} \tag{13}$$

$$S^{\cdot} = \left[\frac{\partial S}{\partial X}\right]^T X^{\cdot} = \left[\frac{\partial S}{\partial Ipv}\right]\left(-\frac{Vo}{L}(1-u) + \frac{Vpv}{L}\right) \tag{14}$$

A description of the first term can be found in (15).

$$\left[\frac{\partial S}{\partial Ipv}\right] = \frac{1}{V_{pv}} + \frac{q}{N_S n V_T}\frac{\partial Ipv}{\partial Vpv}\ \frac{\partial Vpv}{\partial Ipv} - \frac{\partial Vpv}{\partial Ipv}\ \frac{I_{pv}}{{V_{pv}}^2} \tag{15}$$

The first derivative of I_{PV} is given by (16).

$$\frac{\partial I_{pv}}{\partial V_{pv}} = -\left(\exp\left(\frac{q}{N_s \eta V_t}\right)\right) \cdot \frac{q}{N_s \eta V_t} \cdot I_d < 0 \tag{16}$$

V_{PV} is defined as in (17).

$$V_{pv} = \frac{N_S \eta\ V_T}{q}\ \ln\left(\frac{I_{ph} + I_d - I_{pv}}{I_d}\right) \tag{17}$$

The derivative of (17) can be written as (18).

$$\frac{\partial V_{pv}}{\partial I_{pv}} = -\left(ln\left(\frac{I_d}{I_{ph} + I_d - I_{pv}}\right)\right)\frac{N_S \eta\ V_T}{q} < 0 \tag{18}$$

According to (18), it is obvious that the first term (∂S/(∂Ipv)) has a positive sign, in the next step we have to investigate the second term:

$$\dot{X} = -\left(\frac{V_o}{L}\right)(1 - u) + \left(\frac{V_{pv}}{L}\right) = -\left(\frac{V_o}{L}\right)(1 - u_{ec} - u_{STA}) + \left(\frac{V_{PV}}{L}\right) \tag{19}$$

$$= \frac{V_o}{L}\left(-\lambda\,|S|^{\frac{1}{2}}\,sign(S) - \int \gamma\, sign(S)\right) \tag{20}$$

According to (20), we have (21).

$$S\dot{S} = S\left[\frac{\partial S}{\partial I_{pv}}\right]\frac{V_o}{L}\left(-\lambda\,|S|^{\frac{1}{2}}\,sign(S) - \int \gamma\, sign(S)\right) \tag{21}$$

As a result, we can state that the Lyapunov stability is guaranteed because S and $\dot{S}$ have always different signs.

2.3.2. Super-twisting parameters using the grey wolf optimizer

The GWO algorithm is a swarm intelligence technique inspired by the social hierarchy and coordinated hunting behavior observed in grey wolves. In this metaheuristic approach, solution agents are categorized into four hierarchical levels: Alpha, Beta, Delta, and Omega, representing the best, second-best, third-best, and remaining candidate solutions.

The Alpha agents lead the optimization process by steering the search toward the most promising solution identified so far. Beta and Delta agents reinforce this progression by refining the search trajectory, while Omega agents explore less favorable regions of the solution space. This exploration enhances population diversity and reduces the risk of premature convergence to local optima.

The core optimization mechanism follows three sequential phases: target localization, encirclement, and final attack. These stages are emulated by the gradual convergence of agents toward the global optimum, achieved through the iterative reduction of the distance between candidate solutions and the best-performing individual.

– GWO modelling

To implement the GWO algorithm and execute the optimization process effectively, it is essential to construct a mathematical representation of both the grey wolves' hunting strategy and their social hierarchy [4]. The model defines the social structure of the pack as follows: i) The Alpha (α) corresponds to the current best solution in the population; ii) The Beta (β) represents the second-best candidate; iii) The Delta (δ) denotes the third-ranked solution; and iv) All remaining agents are categorized as Omega (ω).

The collective behavior of these four hierarchical groups α, β, δ, and ω guides the optimization dynamics throughout the search process. Subsequently, the encircling behavior observed in grey wolf hunting is mathematically modeled using a set of equations, which simulate the adaptive positioning of solution agents around a potential optimum.

$$\vec{D} = \left|\vec{C}\cdot\overrightarrow{X_p} - \vec{X}(t)\right| \tag{22}$$

$$\vec{X}(t+1) = \overrightarrow{X_p}(t) - \vec{D}\cdot\vec{A} \tag{23}$$

$\vec{A}$ *and* $\vec{C}$ coefficient vectors, t denotes the current iteration, $\overrightarrow{X_p}$ represents the position of the prey, and $\vec{X}$ indicates the position of a grey wolf. The vectors $\vec{A}$ and $\vec{C}$ are defined as (24) and (25) [13], [24].

$$\vec{A} = 2\,\vec{a}\cdot\overrightarrow{r_1} - \vec{a} \tag{24}$$

$$\vec{C} = 2\,\overrightarrow{r_2} \tag{25}$$

Vectors $\overrightarrow{r_1}$ and $\overrightarrow{r_2}$ are randomly generated, while the coefficient $\vec{a}$ decreases linearly from 2 to 0. Figure 6 demonstrates how to change the positions of elements *α*, *β,* and *δ*, accordingly. To model the hunting strategy within the promising regions of the search space, the (26)-(28) mathematical expressions are used.

$$\overrightarrow{D_\alpha} = \left|\overrightarrow{C_1}\,\overrightarrow{X_\alpha} - \vec{X}\right|, \overrightarrow{D_\beta} = \left|\overrightarrow{C_2}\,\overrightarrow{X_\beta} - \vec{X}\right|, \overrightarrow{D_\delta} = \left|\overrightarrow{C_3}\,\overrightarrow{X_\delta} - \vec{X}\right| \tag{26}$$

$$\begin{cases} \overrightarrow{X_1} = \overrightarrow{X_\alpha} - \overrightarrow{A_1}\left(\overrightarrow{D_\alpha}\right) \\ \overrightarrow{X_2} = \overrightarrow{X_\beta} - \overrightarrow{A_2}\left(\overrightarrow{D_\beta}\right) \\ \overrightarrow{X_3} = \overrightarrow{X_\delta} - \overrightarrow{A_3}\left(\overrightarrow{D_\delta}\right) \end{cases} \tag{27}$$

$$\vec{X}(t+1) = \frac{1}{3}\left(\overrightarrow{X_1} + \overrightarrow{X_2} + \overrightarrow{X_3}\right) \tag{28}$$

$\vec{A}$ is a random vector whose components are independently drawn from a uniform distribution over the interval $[-a, a]$.

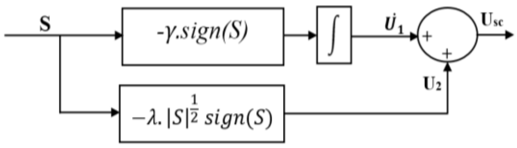

Figure 5. Provides the structure of the STA

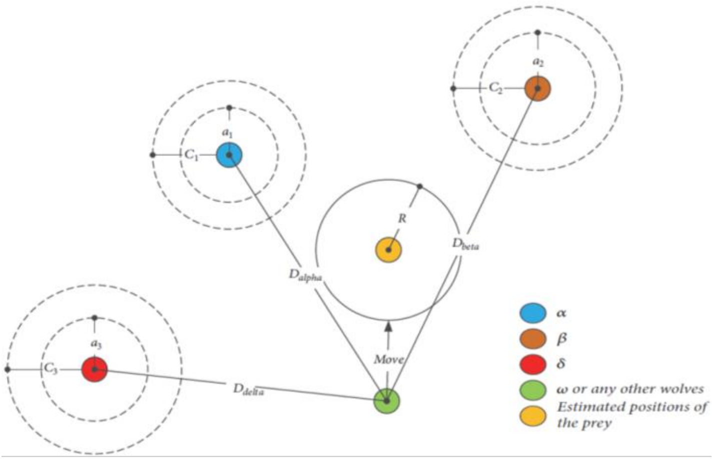

Figure 6. Position update process in grey wolf optimization [25]

3. RESULTS AND DISCUSSION

The MPPT performance of the hybrid STA_GWO algorithm was evaluated through MATLAB/Simulink simulations on a PV system using STP80 modules. The GWO is configured with a population size of 20 agents and a maximum of 30 iterations. Current–voltage and power–voltage curves presented in Figure 3 were generated to assess the algorithm's ability to track and stabilize the MPP under varying conditions. The system employs a boost DC–DC converter with L = 2 mH and C = 330 μF, ensuring ΔI <20% at 20 kHz. The STA_GWO controller, implemented as an external script, adaptively adjusts parameters in real time based on system feedback. Two scenarios were tested: first, under STC, the PV system's dynamic response is shown in Figures 7(a)-7(d), illustrating output power, voltage, and current. The waveforms confirm rapid settling around the MPP with stable and robust tracking. Results demonstrate that the STA_GWO-based MPPT achieves fast convergence, negligible steady-state oscillations, and high energy conversion efficiency, underscoring its effectiveness and reliability for PV systems. In the second scenario, the system was subjected to varying irradiance levels (500, 700, 1000, 400, 600 W/m² at T = 25 °C) to emulate realistic environmental changes. Figures 8(a) and 8(b) show the corresponding dynamic responses Figures 8(b)-8(d) show that the STA_GWO method maintains fast and accurate MPPT with minimal power fluctuation across all irradiance stages, confirming its robustness under rapidly changing solar conditions.

These results highlight the algorithm's exceptional capability to swiftly adjust and precisely follow the MPP under rapidly evolving operating conditions. Furthermore, the controller demonstrates strong robustness against sudden irradiance and temperature variations, maintaining stable tracking performance with minimal oscillations. This behavior confirms its suitability for highly dynamic PV environments and emphasizes its potential for improving overall energy harvesting efficiency.

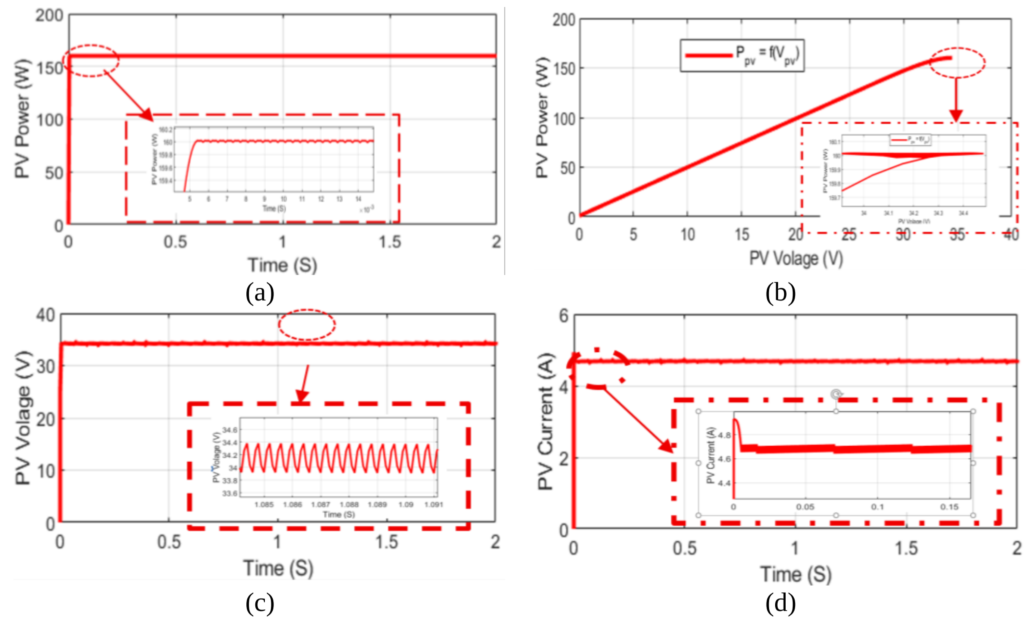

Figure 7. Under STC, the PV system's dynamic response in (a) output PV power, (b) PV curve, (c) PV voltage, and (d) PV current

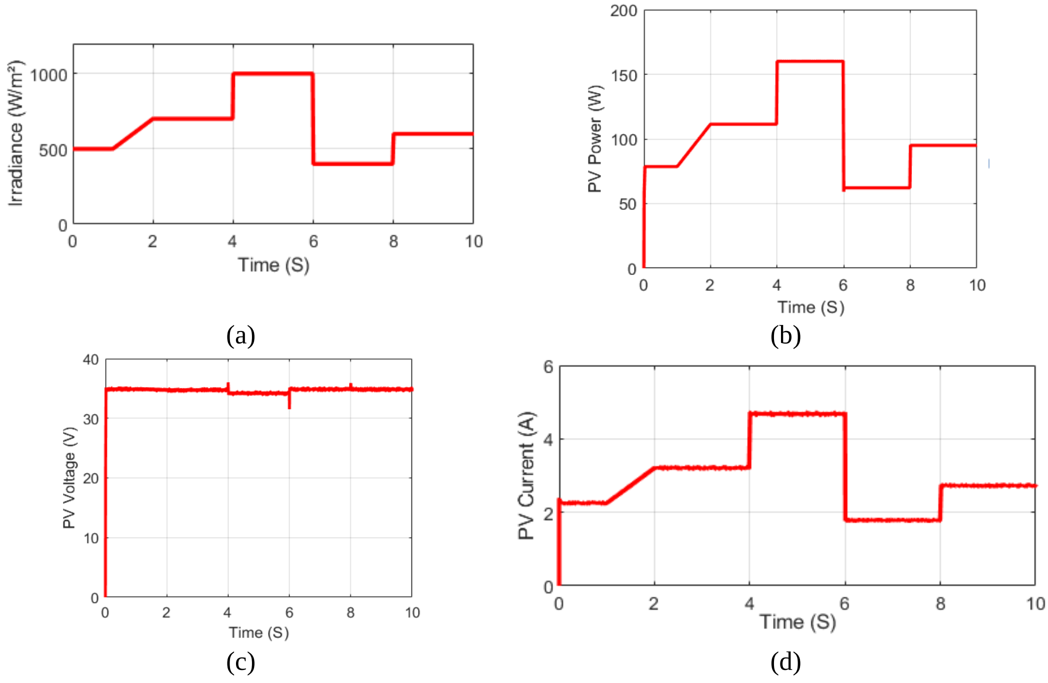

Figure 8. Dynamic response of the PV system under varying irradiance conditions in (a) irradiance, (b) PV power, (c) PV voltage, and (d) PV current under dynamic irradiance

Figure 9 illustrates the dynamic response of SMC_GWO and STA_GWO MPPT algorithms under variable irradiance. Results show that STA_GWO significantly reduces oscillations around the MPP, ensuring stable operation and minimizing power losses during rapid irradiance changes. The method also achieves faster convergence and higher efficiency, confirming its robustness in highly variable solar conditions. Compared to SMC_GWO, STA_GWO demonstrates superior response time and tracking accuracy, positioning it as a notable advancement in MPPT optimization for modern PV systems.

Efficiency evaluation of both techniques considers delivered power, overall efficiency, and RMSE, enabling precise assessment of tracking speed, stability, and accuracy. Table 2 provides averaged statistical results across irradiance levels, while Figure 10 highlights improved tracking efficiency with STA_GWO. Overall, STA_GWO consistently outperforms SMC_GWO under fast-changing irradiance profiles.

$$\eta = \frac{O_{PV}}{R_{PV}} \tag{29}$$

$$\text{RMSE} = \sqrt{\frac{\sum_{i=1}^{n_r}(R_{PV}-O_{PV})^2}{n_r}} \tag{30}$$

Table 2. Efficiency analysis for MPPT algorithms under various irradiance levels

Irradiation (W/m²)		500	700	1000	400	600
Period (S)		[0 1]	[2 4]	[4 6]	[6 8]	[8 10]
Reel Ppv (W) (R_{PV})		78.59	111.38	160	62.20	94.98
Obtained Power (W) (O_{PV})	SMC	77.95	110.47	158.71	61.67	94.23
	STA	78.07	110.65	158.95	61.79	94.37
Efficiency (η)	SMC	99.1856	99.1829	99.1937	99.1479	99.2103
	STA	99.3383	99.3445	99.3437	99.3408	99.3577
RMSE	SMC			0.86547097		
	STA			0.69942833		

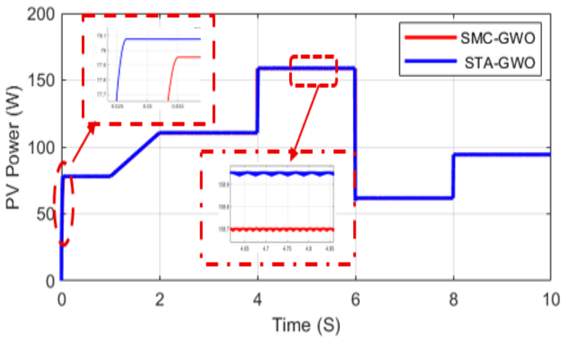

Figure 9. PV power under varying irradiance

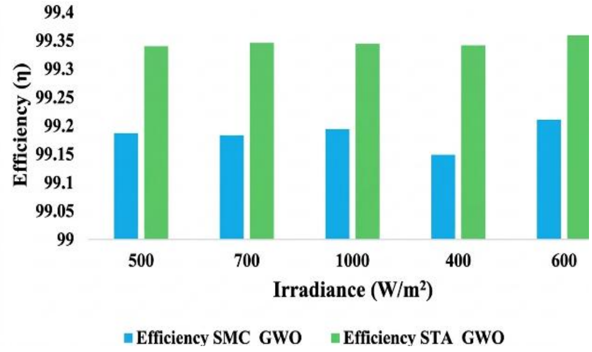

Figure 10. Average tracking efficiency of two MPPT techniques

4. CONCLUSION

This study presents and evaluates a novel MPPT algorithm integrating a second-order sliding mode control-based STA with the GWO metaheuristic to enhance PV system efficiency under variable irradiance conditions within a Simulink simulation framework to improve MPPT performance. The STA reduces chattering and improves accurate tracking of the maximum power point under dynamic environmental conditions and rapid irradiance variations. The GWO algorithm fine-tunes controller parameters, improving robustness and stability of the PV system control loop. MATLAB/Simulink results show that the proposed STA_GWO outperforms conventional SMC_GWO MPPT in comparison with the classical method. Tracking efficiency is increased (SMC_GWO: 99.19%; STA_GWO: 99.34%) with reduced power oscillations, enhancing energy extraction and leading to improved energy harvesting performance under highly fluctuating weather conditions in real operating scenarios. Overall, the hybrid approach improves tracking accuracy, robustness, and chattering reduction compared with existing methods for photovoltaic applications with enhanced overall system performance. Future work will focus on the real-time experimental implementation of these techniques.

FUNDING INFORMATION

Authors state no funding involved.

AUTHOR CONTRIBUTIONS STATEMENT

This journal uses the Contributor Roles Taxonomy (CRediT) to recognize individual author contributions, reduce authorship disputes, and facilitate collaboration.

Name of Author	C	M	So	Va	Fo	I	R	D	O	E	Vi	Su	P	Fu
Slimane Hadji	✓	✓	✓	✓	✓	✓	✓	✓	✓	✓			✓	
Said Aissou			✓	✓		✓	✓			✓	✓	✓		
Abdelhakim Belkaid	✓	✓		✓		✓	✓		✓		✓	✓		

C : **C**onceptualization
M : **M**ethodology
So : **So**ftware
Va : **Va**lidation
Fo : **Fo**rmal analysis
I : **I**nvestigation
R : **R**esources
D : **D**ata Curation
O : Writing - **O**riginal Draft
E : Writing - Review & **E**diting
Vi : **Vi**sualization
Su : **Su**pervision
P : **P**roject administration
Fu : **Fu**nding acquisition

CONFLICT OF INTEREST STATEMENT

Authors state no conflict of interest.

DATA AVAILABILITY

All data underpinning the findings of this study are available from the corresponding author, [SA], upon reasonable request.

REFERENCES

[1] L. Zaghba *et al.*, "Enhancing grid-connected photovoltaic system performance with novel hybrid MPPT technique in variable atmospheric conditions," *Scientific Reports*, vol. 14, no. 1, p. 8205, Apr. 2024, doi: 10.1038/s41598-024-59024-4.

[2] H. Djoudi *et al.*, "Simulation and experimental investigation into a photovoltaic and fuel cell hybrid integration power system for a typical small house application," *Electric Power Components and Systems*, vol. 48, no. 14–15, pp. 1598–1613, Sep. 2020, doi: 10.1080/15325008.2020.1857471.

[3] A. Berboucha, K. Djermouni, K. Ghedamsi, E. Amirouche, S. Aissou, and D. Aouzellag, "Sliding mode control of a photovoltaic water pumping system," in *Proceedings of the 3rd International Electronic Conference on Processes,* Basel, Switzerland, May 2024, p. 48. doi: 10.3390/proceedings2024105048.

[4] R. Rouas, M. Sibrahim, S. Aissou, and S. Haddad, "Sustainable energy empowerment in remote regions wind-solar system with intelligent management," *International Journal of Power Electronics and Drive Systems (IJPEDS)*, vol. 16, no. 1, pp. 86–95, Mar. 2025, doi: 10.11591/ijpeds.v16.i1.pp86-95.

[5] A. Elyazid, A. said, N. Benyahia, A. Belkaid, A. Berboucha, and K. Ghedamsi, "Intelligent management and optimization of renewable sources for remote off-grid areas," *Journal Electrical Systems*, vol. 21, no. 1. pp. 24–37, 2025.

[6] E. Mohammadi, M. Alizadeh, M. Asgarimoghaddam, X. Wang, and M. G. Simoes, "A review on application of artificial intelligence techniques in microgrids," *IEEE Journal of Emerging and Selected Topics in Industrial Electronics*, vol. 3, no. 4, pp. 878–890, Oct. 2022, doi: 10.1109/JESTIE.2022.3198504.

[7] F. F. Ahmad, C. Ghenai, A. K. Hamid, and M. Bettayeb, "Application of sliding mode control for maximum power point tracking of solar photovoltaic systems: a comprehensive review," *Annual Reviews in Control*, vol. 49, pp. 173–196, 2020, doi: 10.1016/j.arcontrol.2020.04.011.

[8] K. H. Chao and M. N. Rizal, "A hybrid MPPT controller based on the genetic algorithm and ant colony optimization for photovoltaic systems under partially shaded conditions," *Energies*, vol. 14, no. 10, p. 2902, May 2021, doi: 10.3390/en14102902.

[9] C. Ben Regaya, H. Hamdi, F. Farhani, A. Marai, A. Zaafouri, and A. Chaari, "Real-time implementation of a novel MPPT control based on the improved PSO algorithm using an adaptive factor selection strategy for photovoltaic systems," *ISA Transactions*, vol. 146, pp. 496–510, Mar. 2024, doi: 10.1016/j.isatra.2023.12.024.

[10] L. Xu, R. Cheng, Z. Xia, and Z. Shen, "Improved particle swarm optimization (PSO)-based MPPT method for PV string under partially shading and uniform irradiance condition," in *2020 Asia Energy and Electrical Engineering Symposium, AEEES 2020*, 2020, pp. 771–775. doi: 10.1109/AEEES48850.2020.9121377.

[11] K. Xia, Y. Li, and B. Zhu, "Improved photovoltaic MPPT algorithm based on ant colony optimization and fuzzy logic under conditions of partial shading," *IEEE Access*, vol. 12, pp. 44817–44825, 2024, doi: 10.1109/ACCESS.2024.3381345.

[12] K. Guo, L. Cui, M. Mao, L. Zhou, and Q. Zhang, "An improved gray wolf optimizer MPPT algorithm for PV system with bfbic converter under partial shading," *IEEE Access*, vol. 8, pp. 103476–103490, 2020, doi: 10.1109/ACCESS.2020.2999311.

[13] M. W. Guo, J. S. Wang, L. F. Zhu, S. S. Guo, and W. Xie, "An improved grey wolf optimizer based on tracking and seeking modes to solve function optimization problems," *IEEE Access*, vol. 8, pp. 69861–69893, 2020, doi: 10.1109/ACCESS.2020.2984321.

[14] N. Priyadarshi, S. Padmanaban, J. B. Holm-Nielsen, F. Blaabjerg, and M. S. Bhaskar, "An experimental estimation of hybrid ANFIS–PSO-based MPPT for PV grid integration under fluctuating sun irradiance," *IEEE Systems Journal*, vol. 14, no. 1, pp. 1218–1229, Mar. 2020, doi: 10.1109/JSYST.2019.2949083.

[15] A. F. Shalal, M. Aljanabi, and A. N. Al-Shamani, "Modified tracking mechanism of horse optimization method (HOM) based MPPT technique for photovoltaic (PV) systems," *AIP Conference Proceedings*, vol. 3092, no. 1, 2024, doi: 10.1063/5.0200083.

[16] A. T. Naser, K. K. Mohammed, N. F. A. Aziz, K. Kamil, and S. Mekhilef, "Improved coot optimizer algorithm-based MPPT for PV systems under complex partial shading conditions and load variation," *Energy Conversion and Management: X*, vol. 22, p. 100565, Apr. 2024, doi: 10.1016/j.ecmx.2024.100565.

[17] I. Owusu-Nyarko, M. A. Elgenedy, I. Abdelsalam, and K. H. Ahmed, “Modified variable step-size incremental conductance MPPT technique for photovoltaic systems,” *Electronics (Switzerland)*, vol. 10, no. 19, p. 2331, Sep. 2021, doi: 10.3390/electronics10192331.

[18] Jara, T.T., Salau, A.O., Markus, E.D., Omeje, C.O., Tin, T.T. (2024). Optimization of a fuzzy-based MPPT controller for a PV water pumping system through a PSO-based approach. Mathematical Modelling of Engineering Problems, Vol. 11, No. 9, pp. 2418-2424, doi: 10.18280/mmep.110914.

[19] A. Belkaid, U. Colak, and K. Kayisli, “A comprehensive study of different photovoltaic peak power tracking methods,” in *IEEE Int. Conf. Renewable Energy Research and Applications (ICRERA)*, 2017, pp. 1073–1079. doi: 10.1109/icrera.2017.8191221.

[20] T. Hai, J. M. Zain, and H. Nakamura, “Maximum power point tracking technique based on variable step size with sliding mode controller in photovoltaic system,” *Soft Computing.*, vol. 27, no. 7, pp. 3829–3845, Apr. 2023, doi: 10.1007/s00500-022-07588-6.

[21] Y. El Alami *et al.*, “Design and realization of a descretized PV system with an improved MPPT control for a better exploitation of the PV energy,” *International Journal of Renewable Energy Research*, vol. 14, no. 2, 2024.

[22] A. Feddaoui, L. Farah, A. Benretem, M. A. Djehaf, and Y. Djeriri, “Enhanced control of DFIG-based wind turbine using hybrid fuzzy super-twisting sliding mode control for improved power quality and robustness,” *Journal of Engineering and Technology for Industrial Applications*, vol. 12, no. 57, pp. 628–636, 2026, doi: 10.5935/jetia.v12i57.2920.

[23] A. Zemmit *et al.*, “GWO and WOA variable step MPPT algorithms-based PV system output power optimization,” *Scientific Reports*, vol. 15, no. 1, p. 7810, Mar. 2025, doi: 10.1038/s41598-025-89898-x.

[24] S. K.T., V. Reddy, and A. Robinson, “An innovative grey wolf optimizer with Nelder–Mead search method based MPPT technique for fast convergence under partial shading conditions,” *Sustainable Energy Technologies and Assessments*, vol. 59, p. 103412, Oct. 2023, doi: 10.1016/j.seta.2023.103412.

[25] R. Salgotra, U. Singh, and S. Sharma, “On the improvement in grey wolf optimization,” *Neural Computing and Applications*, vol. 32, no. 8, pp. 3709–3748, Apr. 2020, doi: 10.1007/s00521-019-04456-7.

BIOGRAPHIES OF AUTHORS

Slimane Hadji is a teacher in the Automatic, Telecommunications, and Electronic Department, at Bejaia University. Was born in 1975 in Algeria, received an engineering degree in 1992 from the University of Bejaia, and a Ph.D. degree from Setif University, Algeria. Researcher in research laboratories: LEPCI (Setif) and LIAS (Poitiers-France), then LTII (Bejaia). Topics of research: renewable energies, control systems, PV energy, power systems, and artificial Intelligence. He can be contacted at email: slimane.hadji@univ-bejaia.dz.

Said Aissou was born in Algeria in 1984. He is currently a teacher in the Science and Technology Department and conducts research activities at the Laboratory of Renewable Energy Mastery (LMER). He studied at the University of Bejaia, Algeria, where he received his master's degree in electrical engineering in 2012 and later got his Ph.D. in electrical engineering from the same university in 2016. His research interests include renewable energy integration, power system analysis, and electric vehicles. He can be contacted at email: said.aissou@univ-bejaia.dz.

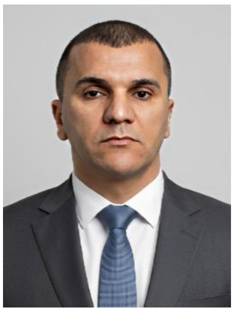

Abdelhakim Belkaid was born in Bejaia, Algeria. He received a B.Sc. degree and a magister's degree from the University of Bejaia, Algeria, in 1998 and 2004, respectively, and a doctorate degree in 2015 in Electrical Engineering from Setif University, Algeria. Currently, he is a professor and the deputy head of the ATE Department, Bejaia University, Algeria. His research interests include: wind and solar energy, power electronics, DC/DC converters, and renewable energy integration. He can be contacted at email: abdelhakim.belkaid@univ-bejaia.dz.